FeCycle: Attempting an iron biogeochemical budget from a mesoscale SF_6 tracer experiment in unperturbed low iron waters

P. W. Boyd,[1] C. S. Law,[2] D. A. Hutchins,[3] E. R. Abraham,[2] P. L. Croot,[4] M. Ellwood,[5] R. D. Frew,[6] M. Hadfield,[2] J. Hall,[5] S. Handy,[7,8] C. Hare,[3] J. Higgins,[7] P. Hill,[2] K. A. Hunter,[6] K. LeBlanc,[3] M. T. Maldonado,[9] R. M. McKay,[10] C. Mioni,[7] M. Oliver,[2] S. Pickmere,[5] M. Pinkerton,[2] K. Safi,[5] S. Sander,[6] S. A. Sanudo-Wilhelmy,[11] M. Smith,[2] R. Strzepek,[6] A. Tovar-Sanchez,[12] and S. W. Wilhelm[7]

Received 22 February 2005; revised 17 October 2005; accepted 2 November 2005; published 31 December 2005.

[1] An improved knowledge of iron biogeochemistry is needed to better understand key controls on the functioning of high-nitrate low-chlorophyll (HNLC) oceanic regions. Iron budgets for HNLC waters have been constructed using data from disparate sources ranging from laboratory algal cultures to ocean physics. In summer 2003 we conducted FeCycle, a 10-day mesoscale tracer release in HNLC waters SE of New Zealand, and measured concurrently all sources (with the exception of aerosol deposition) to, sinks of iron from, and rates of iron recycling within, the surface mixed layer. A pelagic iron budget (timescale of days) indicated that oceanic supply terms (lateral advection and vertical diffusion) were relatively small compared to the main sink (downward particulate export). Remote sensing and terrestrial monitoring reveal 13 dust or wildfire events in Australia, prior to and during FeCycle, one of which may have deposited iron at the study location. However, iron deposition rates cannot be derived from such observations, illustrating the difficulties in closing iron budgets without quantification of episodic atmospheric supply. Despite the threefold uncertainties reported for rates of aerosol deposition (Duce et al., 1991), published atmospheric iron supply for the New Zealand region is ~50-fold (i.e., 7- to 150-fold) greater than the oceanic iron supply measured in our budget, and thus was comparable (i.e., a third to threefold) to our estimates of downward export of particulate iron. During FeCycle, the fluxes due to short term (hours) biological iron uptake and regeneration were indicative of rapid recycling and were tenfold greater than for new iron (i.e. estimated atmospheric and measured oceanic supply), giving an "*f*e" ratio (uptake of new iron/uptake of new + regenerated iron) of 0.17 (i.e., a range of 0.06 to 0.51 due to uncertainties on aerosol iron supply), and an "F*e*" ratio (biogenic Fe export/uptake of new + regenerated iron) of 0.09 (i.e., 0.03 to 0.24).

Citation: Boyd, P. W., et al. (2005), FeCycle: Attempting an iron biogeochemical budget from a mesoscale SF_6 tracer experiment in unperturbed low iron waters, *Global Biogeochem. Cycles*, *19*, GB4S20, doi:10.1029/2005GB002494.

1. Introduction

[2] There is now conclusive evidence of the key role of iron supply in mediating a wide range of biogeochemical processes [*Morel and Price*, 2003]. Iron supply controls many aspects of algal physiology [*Boyd*, 2002a], alters

[1]National Institute of Water and Atmosphere Centre for Chemical and Physical Oceanography, Department of Chemistry, University of Otago, Dunedin, New Zealand.
[2]National Institute of Water and Atmosphere, Greta Point, Wellington, New Zealand.
[3]College of Marine Studies, University of Delaware, Lewes, Delaware, USA.
[4]Leibniz-Institut für Meereswissenschaften (IFM-GEOMAR), Kiel, Germany.
[5]National Institute of Water and Atmosphere, Hillcrest, Hamilton, New Zealand.
[6]Department of Chemistry, University of Otago, Dunedin, New Zealand.
[7]Department of Microbiology, University of Tennessee, Knoxville, Tennessee, USA.
[8]Now at College of Marine Studies, University of Delaware, Lewes, Delaware, USA.
[9]Department of Earth and Ocean Sciences, University of British Columbia, Vancouver, British Columbia, Canada.
[10]Department of Biological Sciences, Bowling Green State University, Bowling Green, Ohio, USA.
[11]Marine Sciences Research Center, Stony Brook University, Stony Brook, New York, USA.
[12]Instituto Mediterraneo de Estudios Avanzados (IMEDEA), Mallorca, Spain.

0886-6236/05/2005GB002494

phytoplankton species composition [*Bruland et al.*, 2001], and controls aspects of the physiology of microzooplankton [*Chase and Price*, 1997] and heterotrophic bacteria [*Tortell et al.*, 1996]. Taken together, the influence of iron on the biota will impact the elemental cycles of carbon, sulfur, silicon and nitrogen by altering downward POC export [*Boyd et al.*, 2004a], DMSP and DMS production [*Turner et al.*, 2004]; algal nutrient stoichiometry [*Hutchins and Bruland*, 1998], and new production rates [*Brzezinski et al.*, 2003], respectively. All of these processes are feedbacks that may influence climate [*Boyd and Doney*, 2003]. Thus, it is necessary to better understand the biogeochemical iron cycle in the ocean.

[3] Previous studies of oceanic iron biogeochemistry have focused on either geochemical or biological aspects. The former include global data synthesis and modeling [*Johnson et al.*, 1997]; geochemical iron budgets [*Martin et al.*, 1989; *Sherrell and Boyle*, 1992; *de Baar et al.*, 1995]; and coupled iron geochemical and general circulation modeling [*Fung et al.*, 2000; *Archer and Johnson*, 2000; *Parekh et al.*, 2004]. In contrast, the latter have attempted to quantify the contribution of the biota in iron budgets and their geochemical role [*Bowie et al.*, 2001; *Tortell et al.*, 1999; *Price and Morel*, 1998]. These geochemically and biologically based studies have provided insights into iron biogeochemistry such as the key role played by ligands in controlling deep water iron concentrations [*Johnson et al.*, 1997; *Archer and Johnson*, 2000], and the importance of biological iron recycling [*Hutchins et al.*, 1993; *Bowie et al.*, 2001], respectively. However, there has so far been little effort to construct iron budgets that combine both geochemical and biological approaches; these are needed to resolve issues such as the relative contribution of new versus recycled iron to budgets [*Fung et al.*, 2000]. Moreover, previous iron budgets have had to rely on the collation of data from a wide range of sources ranging from algal laboratory culture studies [*Price and Morel*, 1998] to ocean physics [*de Baar et al.*, 1995]. Our understanding of iron biogeochemistry has been hindered by the absence of key budget terms, such as iron remineralization dynamics and the iron composition of mixed layer and sinking particles in the upper ocean [*Wu and Boyle*, 2002; *Fung et al.*, 2000], and the uncertainties introduced into budgets by reliance on estimates from disparate sources.

[4] So far, many of our insights into iron biogeochemistry have come from shipboard and mesoscale iron perturbation experiments [*Rue and Bruland*, 1997; *Bowie et al.*, 2001; *Croot et al.*, 2001]. However, clearly there is now a need for an experimental approach that measures concurrently the pools and fluxes within the biogeochemical iron cycle without perturbing the HNLC condition. The tracer sulphur hexafluoride (SF_6) provides an appropriate tool to conduct such an experiment, and has been used to explore the physics and chemistry of the unperturbed ocean during eddy studies [*Law et al.*, 2001]. The use of the SF_6 tracer, along with the timely advent of new approaches such as iron bioreporters [*Mioni et al.*, 2003] and a trace metal clean wash to remove extracellularly bound iron from particles [*Tovar-Sanchez et al.*, 2003], provide an appropriate "technological" platform for such a study.

[5] Our experiment, FeCycle, took place over 10 days in summer 2003 within an unperturbed (i.e., no iron addition) SF_6 labeled patch of HNLC ocean SE of New Zealand. The aim of FeCycle was to obtain concurrent measurements of the key sources and sinks of new iron to the surface mixed layer, and also estimates of biological iron uptake and recycling within the SF_6 labeled waters. This overview (1) provides a broader temporal and spatial context for the FeCycle study using remotely sensed atmospheric and oceanic observations and (2) summarizes and synthesizes the main findings of FeCycle. The latter rely on the construction of iron biogeochemical budgets on two timescales (hours, days) for the surface ocean from detailed studies in the FeCycle special section. They focus on: mixed layer and sinking particulate iron dynamics [*Frew et al.*, 2005], iron bioavailability to heterotrophic bacteria [*Mioni et al.*, 2005], iron acquisition mechanisms by plankton [*Maldonado et al.*, 2005], algal iron dynamics [*McKay et al.*, 2005], and the role of the microbial foodweb in iron recycling [*Strzepek et al.*, 2005]. Other data are provided on upper ocean physics and chemistry from P. L. Croot et al. (The effects of physical forcing on iron chemistry and speciation during the FeCycle experiment in the South West Pacific, submitted to *Marine Chemistry*, 2005) (hereinafter referred to as Croot et al., submitted manuscript, 2005).

2. Study Site and Methods

[6] Prior to the FeCycle voyage we identified potential sites SE of New Zealand that had HNLC characteristics (Figure 1a). Site selection was refined to one (S. Mooring site, Figure 1a) as it had the most appropriate physical conditions (e.g., away from eddy activity) for a mesoscale tracer release. Site suitability was tested during a survey from 30 January to 1 February 2003, which comprised XBT releases interspersed with CTD casts to 1 km depth. Underway sampling from pumped seawater supply (5 m depth) provided maps of temperature, salinity (Seabird thermosalinograph), chlorophyll (Turner fluorometer), photosynthetic competence (F_v/F_m) [after *Boyd and Abraham*, 2001], dissolved nutrients [*Frew et al.*, 2001] and dissolved iron (DFe) (using a clean tow-fish at 4 m depth after *Bowie et al.* [2001]). The survey found an appropriate site at 178.72°E 46.24°S (auxiliary material[1] table ts01 and Figure 1b), and the SF_6 release commenced at 0200 local time (LT) on 2 February 2003.

[7] The tracer release into the surface mixed layer followed procedures of *Law et al.* [1998] and took 12 hours to add SF_6 over ~49 km^2 (Figure 2a and auxiliary material figure fs01) at a release depth of 7 m. No iron was added along with the SF_6. Immediately following the tracer release, the areal extent of the labeled waters was assessed by underway mapping of the patch. Day 1 of FeCycle was nominally defined as 3 February 2003, and the 10-day study concluded on 12 February.

[8] During FeCycle we conducted several sampling strategies at the patch center (defined as the highest SF_6

[1] Auxiliary material is available at ftp://ftp.agu.org/apend/gb/2005GB002494.

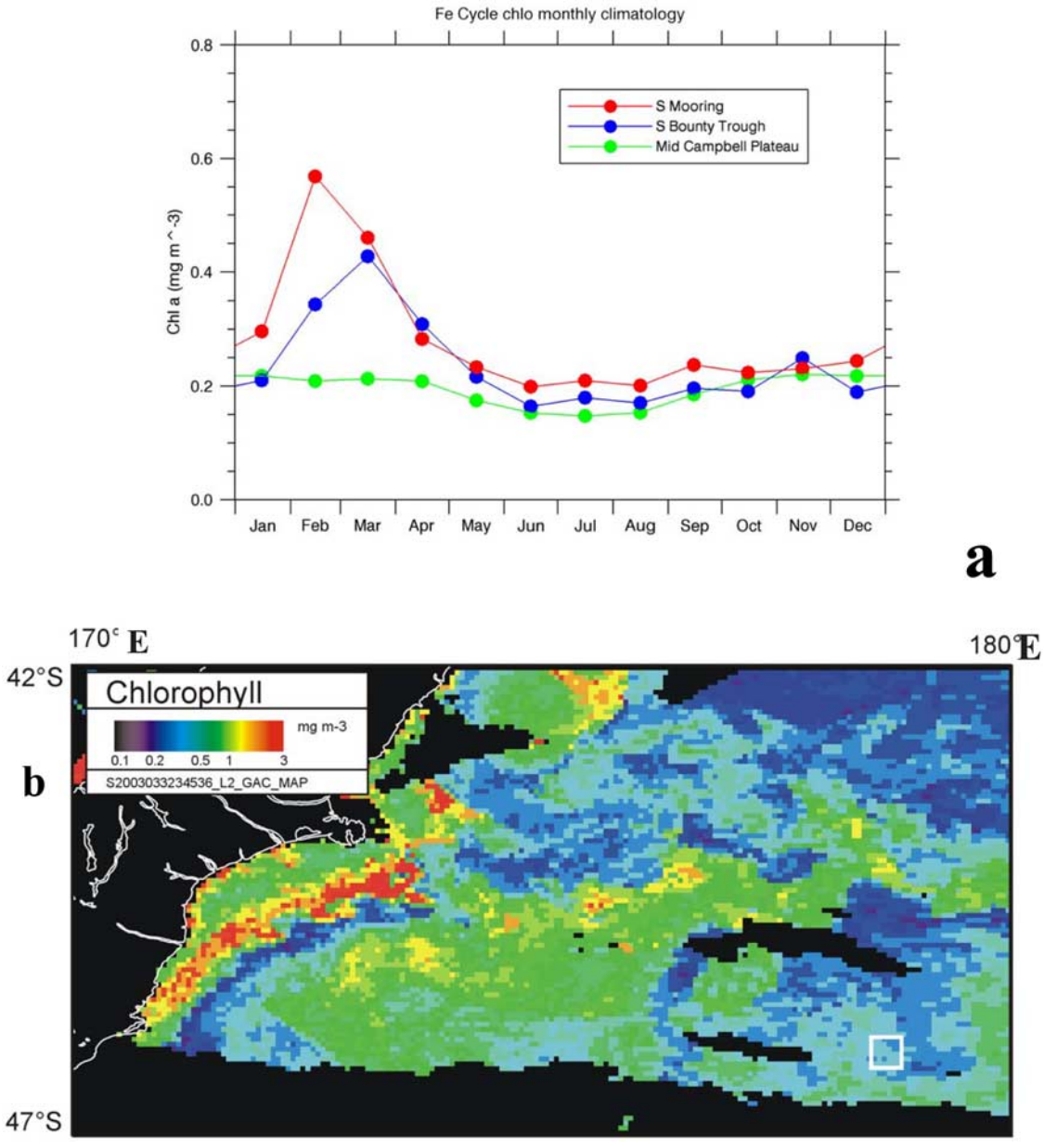

Figure 1. (a) Time series plots of chlorophyll (based on 8-day and monthly SeaWiFs climatology, and the MODIS Aqua time series) for three potential sites SW of New Zealand (denoted by the landmass outlined in Figure 1b) for FeCycle. Concentrations represent mean values for the pixels contained within boxes bounded by 177.5°E to 179.5°E, 47.0°S to 46.0°S (S. Mooring), 173.0°E to 174.0°E, 48.0°S to 47.0°S (S Bounty Trough), and 169.0°E to 170.0°E, 51.0 to 50.0°S (Mid Campbell Plateau). Note that elevated chlorophyll concentrations are observed in late summer only in some years. The reason for this interannual variability is not presently understood [*Boyd et al.*, 2004b]. (b) Location of the site selected for FeCycle (denoted by the white outline at 178.72°E 46.24°S) superimposed upon an 8-day SeaWiFS composite during FeCycle. The OC4V4 algorithm has been validated for this region [*Richardson et al.*, 2004].

concentrations) including budget (on 4 days), depth-resolved (1 day) and diel sampling (2 days). FeCycle concluded with a detailed lateral transect of the patch. Each sampling period was interspersed with overnight mapping of the areal extent of the patch and concurrent sampling of lateral gradients in upper ocean properties. Water sampling on budget days took place at one depth (20 m) and shortly after local dawn when nighttime convective overturn would ensure a truly "mixed" layer for several hours [*MacIntyre*, 1998] before any solar heating influenced the structure of the upper ocean [*McNeil and Farmer*, 1995].

[9] All water was obtained using a trace-metal clean fish in conjunction with trace-metal clean polyethylene tubing and a Teflon pump [*Hutchins et al.*, 1998] with a plastic pressure logger attached near the underwater intake. This system enabled all samples required for the budget to be

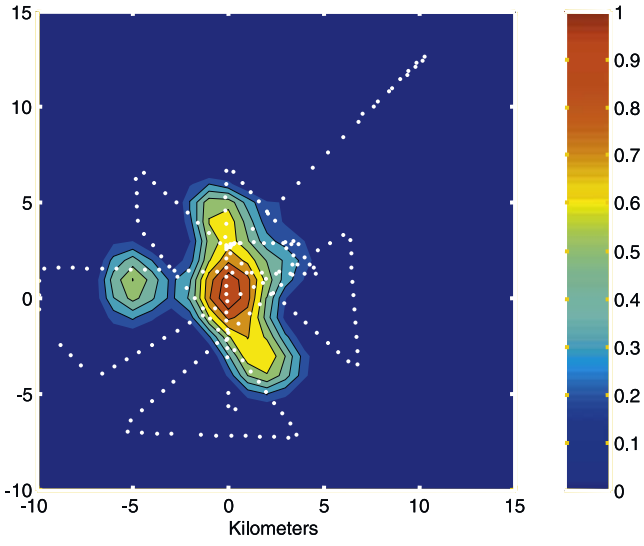

Figure 2a. The areal extent (47 km^2) and shape of the SF_6 labeled FeCycle patch centered on 178.72°E 46.24°S on 3 February 2003 (i.e., directly after the completion of the SF_6 release). The patch is defined as the area with SF_6 concentrations larger than one third of the peak SF_6 concentration (denoted as 1 on the scale bar). White dots represent the individual underway measurements on which the contouring is based.

obtained in <3 hours. Specific details of the sampling and analytical protocols for particulates, phytoplankton, iron chemistry and microbial components of this budget are presented by *Frew et al.* [2005], *Ellwood* [2004], *McKay et al.* [2005], and *Strzepek et al.* [2005], respectively.

[10] Other sampling during FeCycle included measuring particulate iron (PFe) flux exiting the upper ocean, and atmospheric iron deposition into the ocean. Export estimates were obtained by deploying two trace metal "clean" surface-tethered free-drifting sediment trap arrays for 7 days at 80 and 120 m depth [*Frew et al.*, 2005]. Export flux was corrected for Fe contamination, using procedural blanks (20% or less of the PFe fluxes) taken from replicate sediment trap tubes [*Frew et al.*, 2005]. On two occasions, dust was sampled using a filtration unit located on a mast (10 m above sea level) on the bow, on both the outward north-south leg (29/30 January from Wellington, 175°E 41°S) to the FeCycle site, and the return south-north leg (12/13 February). These >24-hour transit times were the only periods sufficient duration to sample aerosols in this relatively low dust deposition region [*Jickells and Spokes*, 2001]. For sampling details, see the auxiliary materials.

[11] Here we present two types of iron budgets: a long-term (i.e., days, focusing on sources of new iron and iron sinks) and a short-term budget (i.e., hours, based on biological iron uptake and recycling). In the latter we have expressed the pools and fluxes as mixed layer column integrals, even though in some cases data were available only from one depth, as they were sampled from a "truly" mixed layer. The short term budgets are "snapshots" in time and space (on days 2, 3, 4 and 7), and have been related to depth-resolved (day 6) and diel (days 5 and 9) sampling [*McKay et al.*, 2005]. On several occasions, due to logistical issues, we have combined data within a daily budget that were obtained on different days during FeCycle; our rationale for this is the relative constancy from day to day in biological properties [*Strzepek et al.*, 2005].

[12] The long term budget comprised four terms; three iron sources (two oceanic and one atmospheric) and one iron sink (downward PFe flux). Estimates of the oceanic terms (vertical diffusive and lateral advective iron supply) were obtained from the exchange between the SF_6 labeled patch and both the surrounding and underlying waters (Figure 2 and auxiliary material figure fs01) and related to horizontal (Croot et al., submitted manuscript, 2005) and vertical gradients (Figure 3) in DFe.

3. Results

3.1. Physical Evolution of the FeCycle Patch

[13] Initial mapping revealed that the patch was coherent, had an areal extent of ~47 km^2 (Figure 2a), and high SF_6 concentrations (>300 fmol L^{-1}, Figure 2b). The surface mixed layer depth, as indicated by a minimum in N^2, the buoyancy frequency, was 40–50 m, although SF_6 was initially restricted to 20 m by shallow isopycnals and deepened over days 1–3 to 40 m (Figure 2b). The subsequent development of vertical variation in the patch extent from day 5 (Figure 2b) restricted estimation of the vertical diffusivity (K_z) from SF_6 profiles to days 1–4 only. This was achieved by fitting second-moment integrals to the SF_6 distribution [*Law et al.*, 2003] from 40 m, to obtain a K_z of 0.66 ± 0.11 cm^2 s^{-1}. This is comparable with estimates from other SF_6 experiments, exceeding K_z estimates from the Southern Ocean, (0.11 ± 0.2 cm^2 s^{-1} [*Law et al.*, 2003]), and equatorial Pacific (0.25 cm^2 s^{-1} [*Law et al.*, 1998]), and intermediate between estimates from the North Atlantic (0.3 ± 0.2 cm^2 s^{-1} [*Kim et al.*, 2005]; 2.93 ± 0.42 cm^2 s^{-1} [*Law et al.*, 2001]). A K_z range of 0.05–3 cm^2 s^{-1} was indirectly estimated from N^2 for FeCycle after day 4 (Croot

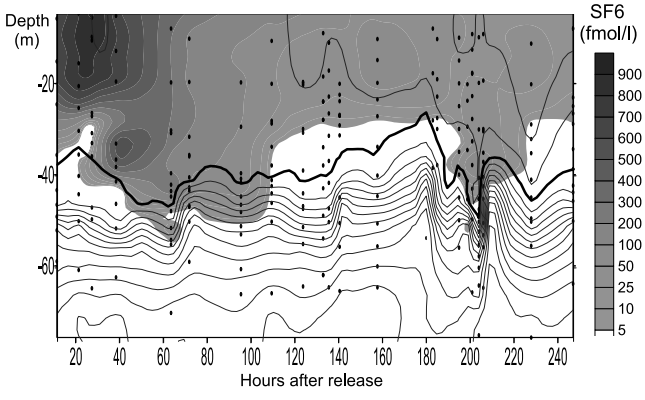

Figure 2b. Time series contour plot of SF_6 concentrations used to define the TLD of the patch (see auxiliary material table ts02). Contouring is based on a series of SF_6 profiles whose depth coverage is indicated by black crosses. Density isopycnals are overlain, with the σ_t = 25.77 isopycnal shown in bold for reference.

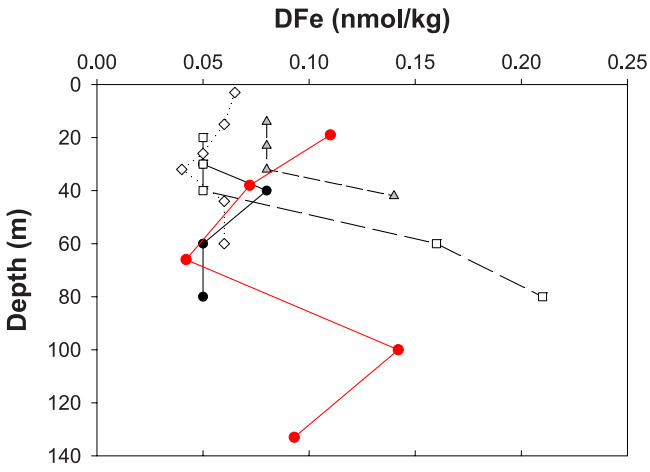

Figure 3. Five seasonal DFe profiles in the upper ocean (analyzed using GFAAS) from 178.30°E 46.30°S. Four profiles are reproduced from *Boyd et al.* [2004b]. Solid circles denote March 2002; open squares denote July 2002; shaded triangles denote November 2002; and open diamonds denote late January 2003 (i.e., at the start of FeCycle). The solid line and solid squares denote a profile at this site in July 2003. The standard error of the mean (n = 3) in each case was <0.03 nmol kg^{-1}.

et al., submitted manuscript, 2005), from a tracer-derived K_z-N^2 parameterization using data presented by *Law et al.* [2003].

[14] From day 5, vertical variability in the patch extent developed in response to the formation of thermal structure and resultant shear in the mixed layer (Figure 2b). The patch developed into a filament of constant width (7 km) and exponentially increasing length ($\gamma = 0.17 \pm 0.03$ d^{-1}(n = 8, R = 0.90), as previously observed in other tracer experiments dominated by strain flow [*Law et al.*, 2003]. As the patch evolved it increased in area by 0.17 d^{-1} to >400 on day 10, and thus may have impacted the iron biogeochemical budgets by both entraining surrounding waters which had slightly different biological signatures (Figure 1b), and altering the physical gradients in the upper ocean (Figure 2b). Changes in tracer layer depths (TLDs) were due to lateral shear events, associated with transient thermal structures within the seasonal mixed layer, whereas the lateral entrainment of water into the patch was mainly driven by shear, strain and rotation.

[15] The impact of lateral entrainment on the FeCycle study is evident from SeaWiFS chlorophyll time series (auxiliary material figure fs02). These data sets indicate that chlorophyll concentrations were typically HNLC (0.2–0.3 μg L^{-1}) on both day 1 and 3 in the vicinity of the patch. However, after day 4, there were higher chlorophyll concentrations in the waters surrounding the patch (up to >1.0 μg chl L^{-1} on day 8) and also inside the patch. These elevated chlorophyll concentrations in the patch were due to either lateral entrainment of waters with higher chlorophyll concentrations or local in situ algal growth. Evidence from FeCycle supports the former mechanism, since there was no significant change in F_v/F_m (0.25) during our study [*McKay et al.*, 2005]; F_v/F_m would have increased prior to any increase in chlorophyll concentrations [*Boyd and Abraham*, 2001]. Similarly, there was no increase in primary production rates (auxiliary material table ts01). Owing to the complex lateral mixing between the patch and the heterogeneous chlorophyll field evident in the surrounding waters (auxiliary material figures fs01 and fs02) entrainment of higher chlorophyll waters cannot be clearly demonstrated. However, application of the patch dilution rate (Croot et al., submitted manuscript, 2005) to the chlorophyll gradient between the patch center and waters outside confirms that lateral entrainment would account for a doubling of chlorophyll in the patch between day 3 and day 8–9, without the necessity for in situ algal growth.

[16] The initial biological and chemical properties of the patch (auxiliary material table ts01) indicate that it was HNLSiLC (high-nitrate low–silicic acid low-chlorophyll [*Dugdale and Wilkerson*, 1998]), rather than HNLC, as is expected in these waters during summer [*Boyd*, 2002b]. The FeCycle patch was dominated by picophytoplankton, and the algal community exhibited low values of F_v/F_m probably due to the picomolar DFe concentrations at this site (Figure 3), and as reported by *Boyd et al.* [1999, 2004b]. In general, there was no significant change in nutrient concentrations, phytoplankton composition, or F_v/F_m during FeCycle [*McKay et al.*, 2005].

3.2. Short-Term Iron Budgets

[17] Four mixed layer budgets were constructed based on size fractions for pico- (0.2–2 μm), nano- (2–5 μm and 5–20 μm) and micro-plankton (>20 μm) after *Sieburth et al.* [1978]. For simplicity, we report only the mixed layer column integrated pool size (from size-fractionated PFe [*Frew et al.*, 2005]), and the fluxes of iron into (biological uptake [*McKay et al.*, 2005]) and out of (biological iron regeneration [*Strzepek et al.*, 2005]) each pool. In each budget, several key trends are consistently observed (Figure 4 and auxiliary material figures fs03 to fs05): (1) the dominance of the bulk PFe pool by particles >20 μm, with a decreasing contribution to total PFe with decreasing size; (2) the greatest contribution to biological iron uptake by the <2-μm fraction, with a decrease in iron uptake generally observed with increasing size; (3) the biologically mediated iron regeneration was comparable for both the heterotrophic bacterial (0.2–0.8 μm) and algal (0.8–8 μm) fractions; (4) the rates of biological iron uptake and regeneration were of the same order; and (5) the pool turnover times for each size class (despite some gaps in each budget) were fastest for the <2-μm fraction (1–3 days based on Fe uptake), and increased with increasing size. Day-to-day variations in the PFe pool size were twofold or less for each size fraction [*Frew et al.*, 2005]. Iron uptake rates for each pool generally showed less than twofold variations (Figure 4 and auxiliary material figures fs03 to fs05), and the results of both grazer-mediated iron regeneration experiments were in particularly close agreement [*Strzepek et al.*, 2005]. In contrast, virally mediated iron regeneration rate estimates ranged from 0.4 to 28 pmol L^{-1} d^{-1} [*Strzepek et al.*, 2005] and were not included within the daily budgets, where steady state was assumed.

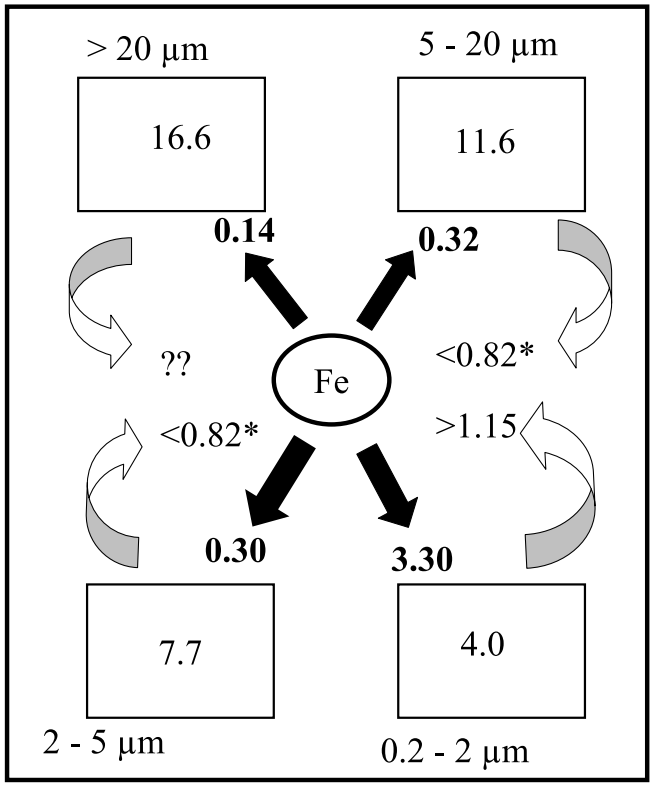

Figure 4. Pools and fluxes for four size classes (0.2–2, 2–5, 5–20, and >20 μm) within the short-term iron budget for the surface mixed layer on day 2 of FeCycle. Units are μmol m^{-2} d^{-1} and μmol m^{-2} for fluxes and pools, respectively. The pools are presented within the box for each size fraction, solid black arrows denote column-integrated iron uptake rates (from seven discrete depths during a 24-hour in situ incubation). The shaded arrows denote iron regeneration rates derived from experiments on days 3 and 5 of FeCycle, using labeled bacteria (0.2–0.8 μm) and labeled phytoplankton (0.8–8 μm). The asterisk denotes that the measured iron regeneration by phytoplankton (0.8–8 μm) straddles both the 2–5 and 5–20 μm size fractions. Double question marks denote that no estimate of herbivory on phytoplankton >20 μm was conducted. Note that PFe data from day 6 are used here.

[18] The trends observed in the short-term budgets can be related to the variability in environmental conditions over FeCycle. With the exception of chlorophyll concentrations, there were only small fluctuations in most of the biological and chemical properties with phytoplankton dominated by <2-μm cells (auxiliary material table ts01). There were twofold ranges in TLDs and incident PAR over the study (auxiliary material table ts02). The variations in TLDs reflected the dynamic nature of the upper 40 m within the seasonal mixed layer that occur over day-week timescales, as much smaller changes in the seasonal mixed layer depth were recorded (Figure 2 caption). Hence the underwater light climate (set by incident irradiance, light attenuance and mixed layer depth) varied little, resulting in less than twofold variations in column-integrated net primary production (auxiliary material table ts01) and iron uptake rates (auxiliary material table ts02). Thus the rates and pools measured during the short-term iron budgets are probably broadly representative of the entire study.

3.3. Long-Term Iron Budget

[19] All iron pools and long-term fluxes measured during FeCycle are presented in Table 1. Lateral advective iron supply was negligible during the 10-day study, and aerosol iron deposition, on the two occasions it was measured, was zero (i.e., identical to the filter blanks). The vertical diffusive supply term was small mainly due to weak vertical gradients in DFe across the pycnocline (0.66 nmol Fe m^{-4} (Figure 3); compared to 0.26 mmol NO_3 m^{-4} [*McKay et al.*, 2005]) as opposed to the low computed values of K_z. The sole loss term from the mixed layer was PFe export flux which was 15- to 30-fold greater than the total iron supply over FeCycle. Despite this apparent imbalance, there were no significant changes in the mixed layer PFe inventory [*Frew et al.*, 2005]. The daily export flux represents around 1% of the PFe inventory in the mixed layer (Table 1), giving a turnover time of the PFe pool of 100 days. The PFe export term can be divided into biogenic (~60%) and lithogenic (~40%) (Table 1). There was no evidence of upwelling (based on density, SF_6 and nutrient data sets) in the vicinity of our site. It appears that although we have measured all of the source and sink terms in the long-term budget there is a marked imbalance between iron supply and removal. Moreover, as most PFe supply will be lithogenic in origin, such as lateral advection or dust deposition [*Jickells and Spokes*, 2001], the budget is also not balanced with respect to biogenic PFe, since it represents 60% of PFe export.

3.4. Dust Activity Prior To and During FeCycle

[20] The supply of iron from dust deposition is often intermittent [*Jickells and Spokes*, 2001] and in the Australasian region is linked to dust storm activity [*Middleton*,

Table 1. Summary of Iron Pools and Long-Term Iron Fluxes (and Standard Deviations) Measured During FeCycle[a]

Property	Measurement
Pools, μmol m^{-2}	
DFe	4 ± 1
PFe	31 ± 7
Fluxes, nmol m^{-2} d^{-1}	
Vertical advective Fe supply	15 ± 3
Lateral advective Fe supply	0 ± 2
Aerosol Fe deposition rate	nd
Downward PFe flux	216 ± 27 to 548 ± 128
Downward lithogenic PFe flux	77 ± 7 to 196 ± 9
Downward biogenic PFe flux	139 ± 31 to 352 ± 123

[a]Inventories of DFe (Figure 3) and PFe [*Frew et al.*, 2005] for the surface mixed layer. The lateral exchange of DFe between the patch (surface mixed layer) and the surrounding waters was based on a K_y estimated from the strain rate of the SF_6 labeled patch and DFe data from a lateral survey of the patch (Croot et al., submitted manuscript, 2005). The vertical diffusive supply was derived from the Fe gradient across the pycnocline (Figure 3) and a K_z from *Law et al.* [2003]. The lithogenic contribution was calculated from an Fe:Al crustal ratio (molar) of 0.18 (based on analysis of Australian dust samples [*Frew et al.*, 2005]). Here nd denotes "no data."

1984]. Between 1 January 2003 and 12 February 2003 there was evidence, from environmental monitoring stations in Australia [*McTainsh*, 1998], of 13 dust events in the arid and semi-arid regions of Australia (auxiliary material table ts03). Backward air mass trajectory analysis indicates that the provenance of hypothetical air parcels passing through the FeCycle site (FeCycle was from year days 34–43) was mainly marine from polar (year days 25, 26, 35–39) or subpolar (year days 26–43) regions south or west of this site (Figure 5). On year days 32 and 33, and 40 to 43, there was evidence of air that had previously transitted over subtropical waters passing through the FeCycle site. There were also several occasions (year days 27, 32–34, 38 and 40) when air from over the Australian subcontinent was subsequently transported in the vicinity of our site (Figure 5). Moreover, on year day 33 there was evidence of several dust storms in eastern Australia (auxiliary material table ts03), and on year day 37 and 38 of elevated aerosol concentrations to the east of New Zealand that extended over subpolar waters south of the FeCycle site (Figure 6). Both of our dust sampling measurements (year days 29/30 and 44/45) coincided with periods when the provenance of air was from the subpolar regions (Figure 5). It is therefore likely that they were not representative of rates of dust deposition during FeCycle (see Figure 6).

4. Discussion

4.1. How Representative Was FeCycle?

[21] The study site was 45 km north of a site in subpolar waters in which both the biota [*Bradford-Grieve et al.*, 1999], and physico-chemical properties of the upper ocean [*Boyd et al.*, 2004a; *Nodder et al.*, 2005] have been characterized throughout the annual cycle. A comparison of the initial conditions during FeCycle (auxiliary material table ts01) with those from this neighboring site [*Boyd et al.*, 1999, 2004b] are favorable with low DFe concentrations, low F_v/F_m and a picophytoplankton-dominated community. During FeCycle, chlorophyll doubled in the SF_6 labeled waters to 0.6 $\mu g\ L^{-1}$ over 5 to 6 days [*McKay et al.*, 2005]. There is evidence, from the regional chlorophyll climatology, of increased concentrations in late summer (Figure 1a). For the period 1997 to 2000, there is no compelling explanation for this trend, although *Boyd et al.* [2004b] put forward a putative mechanism involving episodic north-south transport of subtropical waters associated with the local bathymetry. Thus conditions during FeCycle are representative for summer in these HNLCLSi waters.

[22] Most of the iron inventories and flux data obtained for both the long- and short-term budgets have not previously been measured in the waters SE of New Zealand. Thus it is difficult to comment on how representative they were. However, it is possible to compare the magnitude of bulk fluxes (such as particulate organic carbon (POC) export flux) measured during FeCycle with other seasons for this site. Our estimate of downward POC export was comparable to fluxes (at a similar depth) in April 1996 [*Nodder and Alexander*, 1999] and January 2000 (S. Nodder, unpublished data, 2002). Furthermore, a comparison of trends in mass and POC export flux at 1.5 km depth from an annual time series indicate that export fluxes in February (i.e., the time period of FeCycle) are similar to those over spring and summer suggesting that our POC fluxes are representative of much of the annual cycle. Given the constancy of the downward mass and POC fluxes over most of the annual cycle [*Nodder et al.*, 2005] it is likely that downward PFe fluxes will be similar over spring and summer, unless there are marked seasonal changes in the Fe:C ratios of settling particles.

[23] Other trends in FeCycle, such as the close coupling of algal growth and herbivory [*Strzepek et al.*, 2005], the constancy of the HNLC condition, and the dominance of small algal cells [*McKay et al.*, 2005] have been previously recorded [*Bradford-Grieve et al.*, 1999; *Boyd et al.*, 1999] suggesting that rapid iron recycling will characterize much of the annual cycle. Temporal trends in DFe profiles at this site indicate that they have a small seasonal amplitude, and weak gradients across the pycnocline (Figure 3). The characteristics of these profiles are similar to that reported in summer for subantarctic waters south of Australia by *Sedwick et al.* [1997]. However, when compared to trends in macronutrients [*McKay et al.*, 2005] the gradients in DFe (0.66 nmol Fe m^{-4}) and nitrate (0.26 mmol NO_3 m^{-4}) supply across the pycnocline during FeCycle yield a molar supply ratio of 2.5×10^{-6} (i.e., several orders of magnitude lower than planktonic Fe:N molar ratios [*Martin et al.*, 1989]. It is not possible to predict how winter overturn will influence the vertical supply of DFe, although the small vertical DFe gradients over the upper 150 m suggest that vertical diffusive supply of iron will remain low over much of the annual cycle.

4.2. Iron Uptake and Recycling: Short-Term Iron Budgets

[24] Iron recycling through the microbial foodweb is reported to take place on a timescale of hours by both micro- [*Barbeau and Moffett*, 2000] and meso-zooplankton [*Hutchins and Bruland*, 1994]. Hence we conducted four daily budgets to measure the fluxes due to iron uptake and regeneration. Despite some missing terms, there are three main trends for each budget: first the >20 μm fraction consistently had the largest PFe pool (97 ± 3% of PFe was lithogenic [*Frew et al.*, 2005]) but the smallest fluxes (iron uptake). In contrast, the 0.2- to 2-μm fraction had the largest fluxes and the smallest PFe pool (68 ± 6% of PFe was lithogenic). The biogenic pool comprised around 15% of total PFe pool, as estimated independently by *Frew et al.* [2005] and *Strzepek et al.* [2005]. Strzepek et al. report that the <2-μm fraction made the largest contribution to this biogenic pool. PFe:POC molar ratios were ~40 for FeCycle

Figure 5. Examples of the main sources of air passing through the FeCycle site in February 2003. Plot I, polar marine; plot II, subpolar marine; plots III and V, Australian coastal/terrestrial; plots IV and VI, subtropical marine. Air mass back trajectories through the FeCycle site were based on heights of 100, 300, 500, 700, 1000, and 1500 m, using HYSPLIT [see *Boyd et al.*, 2004b].

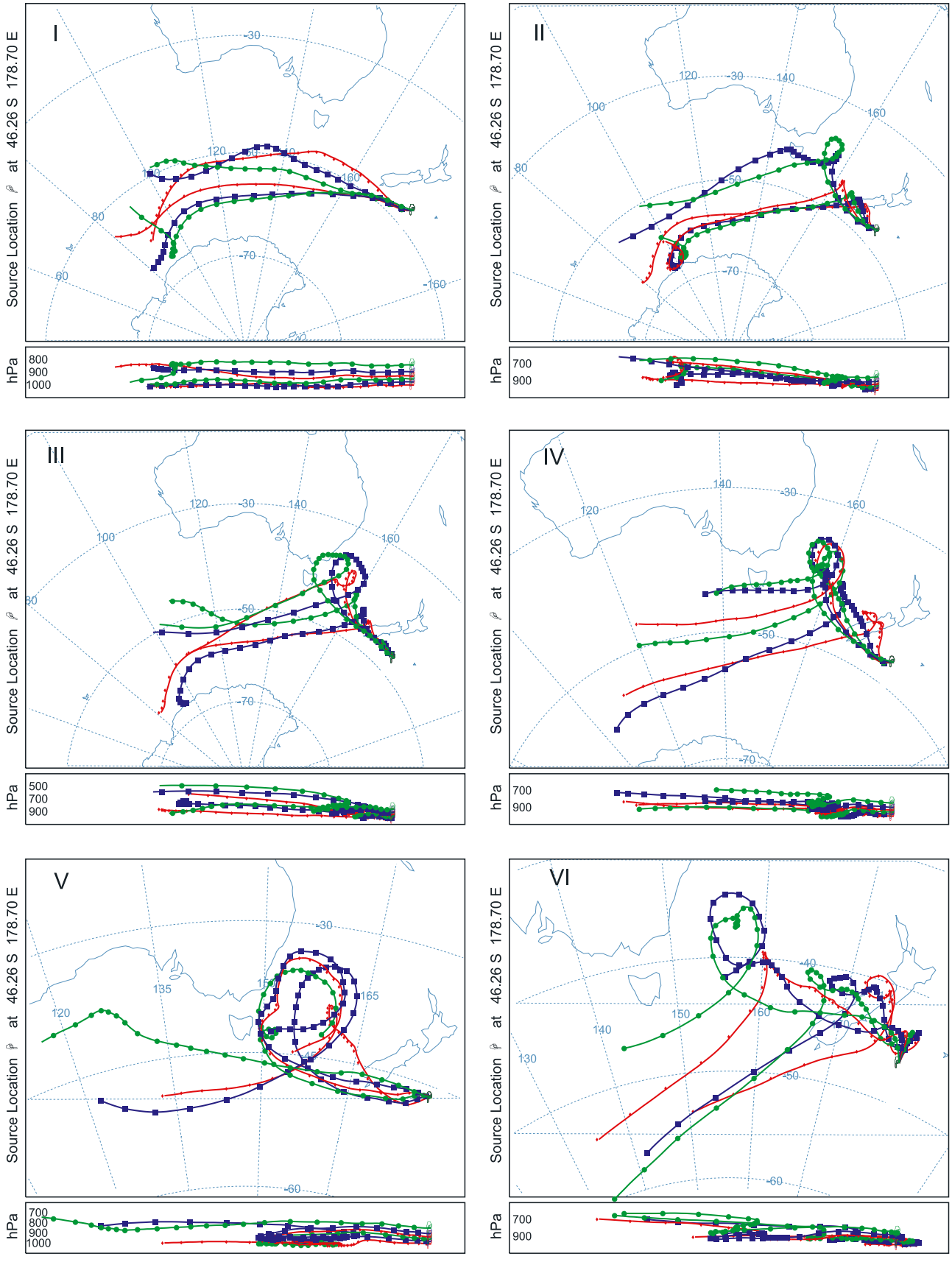
I
II
III
IV
V
VI
Source Location @ at 46.26 S 178.70 E
hPa
800
900
1000
700
900
500
700
900
700
800
900
1000

Figure 5

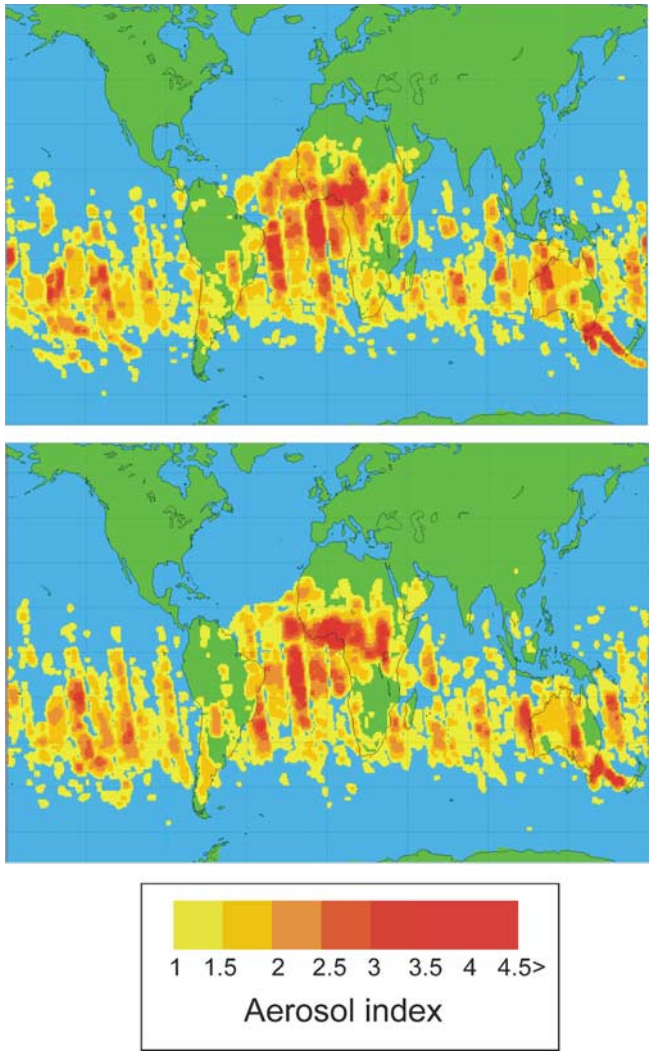

Figure 6. TOMS aerosol index for (top) 6 and (bottom) 7 February 2003 with evidence of elevated aerosol concentrations in the Tasman Sea east of New Zealand. Air mass back trajectory analysis points to potential transport of air masses from both the Tasman Sea and terrestrial Australia on 6 and 7 February.

[*Frew et al.*, 2005], but after correction for the lithogenic component, were 5–6, similar to those for HNLC Southern Ocean waters [*Twining et al.*, 2004a, 2004b].

[25] Second, the uptake of iron in most of the size fractions during FeCycle was comparable to its rate of recycling for each budget day, indicative of active mobilization of a large proportion of the iron in each of the four size fractions. *Bowie et al.* [2001] also reported this trend for the SOIREE mesoscale iron enrichment in the Southern Ocean, suggesting that regardless of the size of the iron inventory there is always rapid recycling. During FeCycle, both the herbivore and bacterivore-mediated rates of regeneration were similar and relatively constant (15–20 pmol L^{-1} d^{-1}), whereas virally mediated iron regeneration ranged by 70-fold (0.4–28 pmol L^{-1} d^{-1}) [*Strzepek et al.*, 2005]. The grazer-mediated iron regeneration rates (33–44 pmol L^{-1} d^{-1}) for FeCycle were comparable to those reported by *Bowie et al.* [2001] (19 pmol L^{-1} d^{-1}, SOIREE), but were fourfold higher than in the HNLC NE subarctic Pacific [*Price and Morel*, 1998].

[26] The third trend during FeCycle was of biogenic pool turnover times for each budget on the order of 1 day (i.e., hours) to weeks, with the fastest turnover times for the cells <2 μm. The PFe pool turnover times are faster (biogenic pool, hours to a few days) after correction for the lithogenic PFe component of the pool for each size class, whereas the lithogenic pools have much longer turnover times of weeks [*Frew et al.*, 2005]. The fast turnover times of the biogenic PFe pools during each of the four budget days of FeCycle are comparable to those reported from both laboratory [*Hutchins et al.*, 1995] and field studies [*Tortell et al.*, 1999; *Bowie et al.*, 2001].

[27] No previous biogeochemical study has constructed multiple iron budgets, based on repeat sampling over several days, and so no other comparisons are available. The consistency in the trends from the FeCycle short-term budgets is probably due to the relatively low fluctuations in environmental conditions that might influence iron biogeochemistry. Such conditions include solar forcing and its impact on photolysis and iron redox cycling [*Barbeau and Moffett*, 2000], photosynthesis [*McNeil and Farmer*, 1995], diel patterns in grazer dynamics [*Fuhrman et al.*, 1985] and viral damage due to photolysis [*Wilhelm et al.*, 1998]. During FeCycle, both daily incident irradiances (27 to 45 mol quanta m^{-2} d^{-1}), and TLDs (25–45 m) ranged by less than twofold, compared with previous voyages in this region where fourfold variations in daily incident irradiances were recorded (P. W. Boyd, unpublished data, 2004).

[28] The balancing of biological iron uptake and regeneration within the "ferrous wheel" [*Kirchman*, 1996] in the mixed layer provides insights into questions raised by *Strom et al.* [2000]: What sets HNLC chlorophyll concentrations at ~0.3 μg L^{-1}, and how is the HNLC condition maintained? Strom et al. suggested that the constancy of the HNLC condition was related to prey switching, i.e., the plastic feeding abilities of microzooplankton that dominate HNLC waters. The tight coupling between iron supply and demand by the microbial foodweb, that is evident from FeCycle, points to a key role of iron in these waters in setting the HNLC condition. The balancing of iron uptake and supply within the "ferrous wheel" we observed raises a further issue: If more iron was supplied to the microbial foodweb, would the wheel spin faster or become larger?

4.3. Sources and Sinks for Iron: Long-Term Budget

[29] The long-term iron budget during FeCycle is characterized by a marked imbalance between the magnitude of iron sources and sinks, with downward PFe export being several orders of magnitude higher than all of the source terms. However, despite this imbalance, there was no change in the mixed layer PFe inventory [*Frew et al.*, 2005], which suggests that we have underestimated the iron supply to the upper ocean. The ability to use the SF_6 tracer to estimate the vertical diffusive and lateral advective iron terms in the budget suggests that both these supply terms

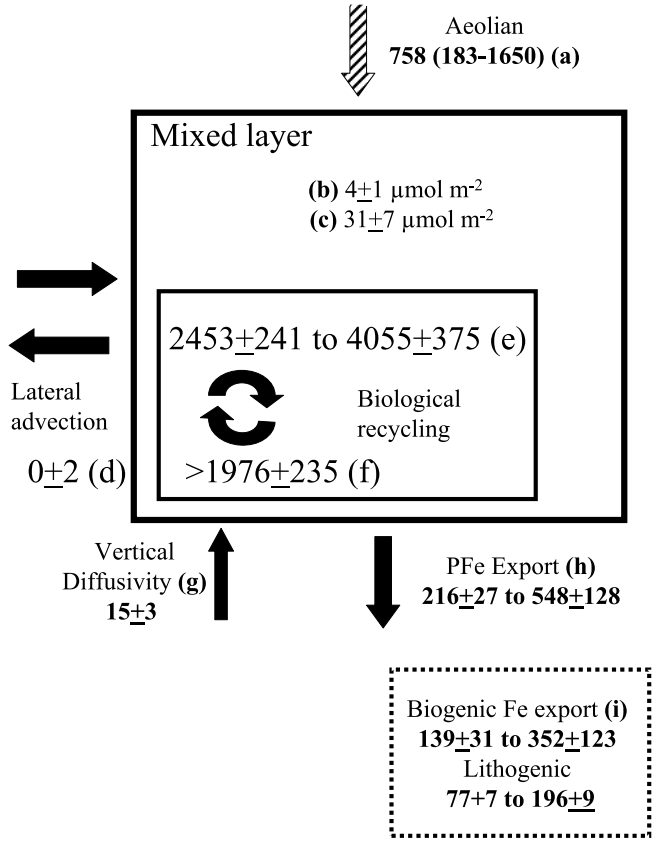

Figure 7. An iron budget for the surface mixed layer during FeCycle. Rates are in nmol m^{-2} d^{-1} and pools in μmol m^{-2}. All terms were measured except for "a," which is represented by a shaded arrow. Term "a" denotes the deposition rate of aerosol iron for the New Zealand region (from *Arimoto et al.* [1990] and scaled for summer dust storm activity after *Middleton* [1984]). The range of rates in parentheses denote the upper and lower bounds on the regional deposition rate from *Jickells and Spokes* [2001] due to the threefold uncertainty for such rates [*Duce et al.*, 1991]; "b" denotes the DFe inventory (from Figure 3); "c" denotes the PFe inventory [*Frew et al.*, 2005]; "d" denotes negligible lateral exchange of DFe between the patch and the surrounding waters; "e" denotes the range (and standard deviation) of biological iron uptake from 4 incubations [*McKay et al.*, 2005]; "f" short term iron regeneration (and standard deviation) by grazers [*Strzepek et al.*, 2005]; "g" denotes the vertical diffusive supply; "h" denotes the range of PFe export (blank corrected) at 80 m depth obtained from two trap arrays [*Frew et al.*, 2005]; and "i" denotes the lithogenic and biogenic PFe export flux.

are robust. The observed weak vertical DFe gradient at our site suggests that even stochastic events such as storms have little potential to vertically supply new iron. In contrast to the estimation of the oceanic iron supply terms, our two measurements of aerosol iron deposition took place on days when air mass trajectory analysis indicates that the provenance of the air near the FeCycle site was marine from the subpolar Southern Ocean. This observation and the indirect evidence, from satellite remote sensing of dust storm activity, indicates that we most likely underestimated aerosol iron supply. Although remotely sensed data provide insights into aerosol deposition prior to and during FeCycle, they cannot yield estimates of dust depositional fluxes during FeCycle.

4.4. Constraining Aerosol Iron Fluxes During FeCycle

[30] To compare the magnitude of the budget terms (for new and recycled iron) measured during FeCycle with that of aerosol iron flux we have cautiously applied published values for the latter. There are dust deposition rates for Australasia from both global data synthesis [*Jickells and Spokes*, 2001] and models [*Jickells et al.*, 2005]. Although measured and modeled deposition rates (10 mg Fe m^{-2} yr^{-1}) for the New Zealand region show relatively good agreement [*Jickells et al.*, 2005], they are expressed as an annual rate to take into account the episodic and intermittent nature of dust supply (compare auxiliary Table ts03). Despite the episodic characteristics of dust deposition events, analysis of dust storm frequency in Australia between 1957 and 1982 by *Middleton* [1984], and of the regional remote sensing (CZCS) aerosol archives by *Stegmann and Tindale* [1999] both point to pronounced seasonality in dust storm activity over Australia. Spring and summer are characterized by up to threefold more dust storms than winter.

[31] Only one detailed study of dust deposition rates in the New Zealand region has taken place: during the SEAREX programme [*Arimoto et al.*, 1990]. This 3-month time series study atop a 20-m tower at an isolated beach site on the North Island of New Zealand (that included concurrent radon measurements to assess the continental influences on the air sampled) provided daily dust deposition rates from Australia (and subsequent aerosol elemental analysis) in winter (June to August). A study of the main dust trajectory routes from Australia to New Zealand, in conjunction with dust core records, suggests that dust deposition rates to northern New Zealand are comparable with those to southern New Zealand [*Hesse*, 1994] where FeCycle took place. Wet and dry iron deposition rates for winter were 303 nmol Fe m^{-2} d^{-1} (mean, no statistics were provided) at this SEAREX site [*Arimoto et al.*, 1990]. This iron deposition rate can be scaled for February, when FeCycle took place, using the monthly dust storm frequency index of *Middleton* [1984]. In winter the average dust storm activity was 34, compared with 85 storms for February, suggesting that the iron supply rate from dust deposition was ~758 nmol Fe m^{-2} d^{-1} during FeCycle. This estimated deposition rate compares with 550 nmol Fe m^{-2} d^{-1} for the New Zealand region from the global synthesis of *Jickells and Spokes* [2001] (derived by dividing their estimate of 0.2 mmol Fe m^{-2} yr^{-1} by 365). It is likely that there will be up to a threefold uncertainty (i.e., 183 to 1650 nmol Fe m^{-2} d^{-1}) on this global depositional estimate [*Duce et al.*, 1991]. All of these estimates are considerably higher than those measured during FeCycle.

4.5. Attempting a Pelagic Fe Biogeochemical Budget

[32] The inclusion of published aerosol iron deposition rates for our region along with the pools and fluxes measured during FeCycle enables the construction of pelagic iron budget (Figure 7). Despite the uncertainties

in estimating aerosol iron fluxes over such short timescales (days) three trends are evident. First, iron supply from the atmosphere is the dominant iron supply term (i.e., 50-fold greater than the oceanic iron supply terms) to the FeCycle site. Second, the estimated rates of aerosol iron deposition are comparable to the downward PFe export observed for FeCycle (Figure 7) which are broadly representative of spring and summer (see section 4.1). Third, the magnitude of new iron supply from both atmospheric and oceanic sources is small relative to that for recycled iron in the mixed layer (Figure 7).

[33] Despite evidence that published regional estimates of aerosol iron flux are comparable to downward PFe export for FeCycle, major imbalances remain when the downward PFe export flux is divided into lithogenic and biogenic PFe (Figure 7). Regardless of how much PFe is supplied to the ocean from dust deposition, very little (<1%) will be biogenic, yet biogenic PFe comprised 60% of the downward PFe flux (Figure 3), but only <20% of the mixed layer PFe inventory [*Frew et al.*, 2005].

[34] *Frew et al.* [2005] suggest that the most compelling mechanism to reconcile these imbalances in both lithogenic and biogenic PFe sources and sinks is the conversion of a large proportion of the deposited lithogenic PFe into biogenic PFe within the mixed layer. This mechanism relies on two factors: the long timescale (weeks) reported for mixed layer residence time of aerosol lithogenic PFe [*Jickells*, 1999; *Croot et al.*, 2004; *Frew et al.*, 2005], and recent evidence of mechanisms for microbes to access mineral iron via dissolution of iron hydroxides [*Yoshida et al.*, 2002; *Borer et al.*, 2005]. Such a pathway for the biota to access lithogenic PFe has implications for the debate regarding the solubility and bioavailability of aerosol iron [see *Jickells and Spokes*, 2001]. It appears that there are now two timescales of iron solubility: instantaneous (hours, driven by physico-chemical mechanisms) and sustained (weeks, driven by microbes and light climate [*Borer et al.*, 2005]). The latter mechanism, by permitting sustained dissolution of aerosol iron on a timescale of weeks, may act as a buffer for iron supply to the upper ocean, to the episodic and intermittent nature of aerosol iron deposition.

4.6. New Versus Regenerated Iron: First Estimates of an "fe" Ratio

[35] At present, techniques to discriminate between new and regenerated iron, such as stable isotopic tracers, are not sufficiently sensitive to compare the relative magnitude of iron supply from these two distinct pools [*Levasseur et al.*, 2004]. However, the fluxes of new and regenerated iron within the SF_6 labeled FeCycle patch enable us to estimate an *f*e ratio (i.e., uptake of new iron/(uptake of new + regenerated iron)) indirectly. The dominant fluxes in our long timescale budget are particulate and based on "new iron," whereas those in the short-term budget are associated with the biota and the dissolved phase, and are mainly based on "regenerated iron." Biological iron uptake was measured during four 24-hour in situ incubations (Figure 7), and provides the term (new + regenerated iron uptake). From Figure 7 the new iron entering the mixed layer is approximately balanced by the PFe exiting the upper ocean each day. Thus, assuming steady state conditions, the new iron entering the upper ocean is 758 nmol m^{-2} d^{-1} (aerosol iron) and 15 nmol m^{-2} d^{-1} (vertical diffusive supply). However, the former term must be corrected for lithogenic iron leaving the mixed layer of 77 to 196 nmol m^{-2} d^{-1}; this is regarded here as a throughput of lithogenic iron comprising 10 to 26% of aerosol iron. The upper bound for the biological uptake of new iron term is 666 nmol m^{-2} d^{-1} (15 + (758 − 77)). Thus the *f*e ratio for FeCycle is 0.17 (696/4055 nmol m^{-2} d^{-1}). The *e* ratio [*Murray et al.*, 1989] can also be derived for the FeCycle study, here defined as the "F*e*" ratio of (biogenic PFe export/uptake of new + regenerated iron), and is 0.09 (352/4055 nmol m^{-2} d^{-1}). Note that the *f*e ratio would be considerably underestimated if these calculations did not take into account the availability of a larger proportion of lithogenic Fe from dust deposition [*Borer et al.*, 2005]. Previously, the availability of new iron from dust was scaled by a solubility factor ranging from 1 to 10% [*Jickells and Spokes*, 2001].

[36] An "*f*e" ratio of 0.17 and an "F*e*" ratio of 0.09 for Fe limited HNLC waters south of New Zealand is comparable to the lower bound of *f* and *e* ratios for the N-limited oligotrophic waters of the subtropical and tropical ocean [*Karl et al.*, 2003]. Although no *f* ratios are available for the FeCycle site, *Varela and Harrison* [1999] report a mean *f* ratio of 0.21 for the HNLC waters of the NE subarctic Pacific. That the *f*e ratio is less than the *f* ratio for HNLC waters is consistent with the widespread iron limitation of the resident phytoplankton in these waters. As for the *f* ratio (see discussion in the work of *Karl et al.* [2003]), the *f*e ratio will "scale positively" with elevated iron supply, such as from episodic events including dust storms. On the basis of the threefold uncertainties on dust supply rates [*Duce et al.*, 1991] the *f*e ratio might range from 0.05 to 0.48 over the annual cycle.

[37] The low *f*e ratio estimated for FeCycle indicates that the fluxes (iron uptake and regeneration) associated with the "ferrous wheel" are almost tenfold greater than the fluxes of "new iron," and are turning over rapidly (hours to days) compared with weeks for the "new iron" particulate phases. *Fung et al.* [2000] attempted to model iron supply and demand for the upper ocean over annual timescales, and constructed DFe budgets including one for the HNLC NE subarctic Pacific. Fung et al. report that even in this relatively low dust deposition region, aerosol iron supply, rather than upwelling and vertical mixing, is the dominant source of new iron. This is consistent with our findings, and despite the rapid turnover times (hours) of this large regenerated iron pool in FeCycle, the year-round observed tight coupling of phytoplankton and micro-grazers suggest that it may be possible to extrapolate these rates into an annual iron budget. The results of FeCycle point to the need to develop, in parallel, a PFe budget, and to consider the transformations between the biogenic and lithogenic pools in detail.

4.7. FeCycle: Implications for Our Understanding of Iron Biogeochemistry

[38] 1. FeCycle has provided the first estimates of the *f*e and F*e* ratios for HNLC waters. As expected, both ratios are lower than *f* ratios for HNLC waters. As iron recycling is dominant, the biogeochemical cycling of iron in the upper ocean is dominated by the biota.

[39] 2. PFe plays a more significant role in iron biogeochemistry than was previously thought, via a putative lithogenic to biogenic transformation pathway for PFe in which >50% of the lithogenic iron deposited from the atmosphere into the ocean is transformed to biogenic iron during its residence (weeks) in the surface mixed layer. There is a pressing need to construct PFe budgets for other oceanic regions (with high aerosol deposition rates).

[40] 3. As the biogeochemical iron cycle is driven by both oceanic and atmospheric events, it is necessary to sample both on appropriate timescales in order to construct budgets. This is particularly difficult to do for the atmosphere which is characterized by intermittent and episodic supply.

[41] 4. Improved understanding of iron biogeochemistry in the open ocean requires the development of new techniques such as: (1) the use of highly sensitive isotopic tracers of Fe fluxes; (2) methods to measure the bioavailability and uptake of actual and specific natural dissolved organic ligand-bound pools (these are needed to supersede existing iron radio-isotope approaches); and (3) long-term, event-resolved dust sampling (moorings).

[42] **Acknowledgments.** Thanks are owed to the officers and crew of the research vessel RV *Tangaroa*, and the personnel at NIWA vessel services. We are grateful to G. McTainsh for access to data from his dust environmental monitoring network. We acknowledge Orbimage and NASA for the availability of satellite images presented here (SeaWiFs and TOMS). This research was funded in part by the New Zealand PGSF Ocean Ecosystems project.

References

Archer, D. E., and K. Johnson (2000), A model of the iron cycle in the ocean, *Global Biogeochem. Cycles*, *14*, 269–279.

Arimoto, R., B. J. Ray, R. A. Duce, A. D. Hewitt, R. Boldi, and A. Hudson (1990), Concentrations, sources and fluxes of Trace elements in the remote marine atmosphere of New Zealand, *J. Geophys. Res.*, *95*, 22,389–22,405.

Barbeau, K., and J. W. Moffett (2000), Laboratory and field studies of colloidal iron oxide dissolution as mediated by phagotrophy and photolysis, *Limnol. Oceanogr.*, *45*, 827–835.

Borer, P. M., B. Sulzberger, P. Reichard, and S. M. Kraemer (2005), Effect of siderophores on the light-induced dissolution of colloidal iron(III) (hydr)oxides, *Mar. Chem.*, *93*, 179–193.

Bowie, A. R., et al. (2001), The fate of added iron during a mesoscale fertilisation in the Southern Ocean, *Deep Sea Res., Part*, 2703–2744.

Boyd, P. W. (2002a), Environmental factors controlling phytoplankton processes in the Southern Ocean, *J. Phycol.*, *38*, 844–861.

Boyd, P. W. (2002b), The role of iron in the biogeochemistry of the Southern Ocean and equatorial Pacific: A comparison of in situ iron enrichments, *Deep Sea Res., Part II*, *49*, 1803–1822.

Boyd, P. W., and E. R. Abraham (2001), Iron-mediated changes in phytoplankton photosynthetic competence during SOIREE, *Deep Sea Res., Part II*, *48*, 2529–2550.

Boyd, P. W., and S. C. Doney (2003), The impact of climate change and feedback processes on the ocean carbon cycle, in *Ocean Biogeochemistry: The role of the ocean carbon cycle in global change*, edited by M. J. R. Fasham, pp. 157–187, Springer, New York.

Boyd, P., J. Laroche, M. Gall, R. Frew, and R. M. L. McKay (1999), Role of iron, light and silicate in controlling algal biomass in subantarctic waters southeast of New Zealand, *J. Geophys. Res.*, *104*, 13,395–13,408.

Boyd, P. W., G. McTainsh, V. Sherlock, K. Richardson, S. Nichol, M. Ellwood, and R. Frew (2004a), The decline and fate of an iron-induced subarctic phytoplankton bloom, *Nature*, *428*, 549–553.

Boyd, P. W., et al. (2004b), Episodic enhancement of phytoplankton stocks in New Zealand subantarctic waters: Contribution of atmospheric and oceanic iron supply, *Global Biogeochem. Cycles*, *18*, GB1029, doi:10.1029/2002GB002020.

Bradford-Grieve, J. M., P. W. Boyd, F. H. Chang, S. Chiswell, M. Hadfield, J. A. Hall, M. R. James, S. D. Nodder, and E. A. Shushkina (1999), Pelagic ecosystem structure and functioning in the Subtropical Front region east of New Zealand in austral winter and spring 1993, *J. Plankton Res.*, *21*, 405–428.

Bruland, I. W., E. L. Rue, and G. J. Smith (2001), Iron and macronutrients in California coastal upwelling regimes: Implications for diatom blooms, *Limnol. Oceanogr.*, *46*, 1661–1674.

Brzezinski, M. A., M. L. Dickson, D. M. Nelson, and R. Sambrotto (2003), Ratios of Si, C and N uptake by microplankton in the Southern Ocean, *Deep Sea Res., Part II*, *50*, 619–633.

Chase, Z., and N. M. Price (1997), Metabolic consequences of iron deficiency in heterotrophic marine protozoa, *Limnol. Oceanogr.*, *42*, 1673–1684.

Croot, P. L., A. R. Bowie, R. D. Frew, M. T. Maldonado, J. A. Hall, K. A. Safi, J. La Roche, P. W. Boyd, and C. S. Law (2001), Persistence of dissolved iron and Fe^{II} in an iron induced phytoplankton bloom in the Southern Ocean, *Geophys. Res. Lett.*, *28*, 3425–3428.

Croot, P. L., P. Streu, and A. R. Baker (2004), Short residence time for iron in surface seawater impacted by atmospheric dry deposition from Saharan dust events, *Geophys. Res. Lett.*, *31*, L23S08, doi:10.1029/2004GL020153.

de Baar, H. J. W., J. T. M. de Jong, D. C. E. Bakker, B. M. Loscher, C. Veth, U. Bathmann, and V. Smetacek (1995), Importance of iron for plankton blooms and carbon dioxide drawdown in the Southern Ocean, *Nature*, *373*, 412–415.

Duce, R. A., et al. (1991), The atmospheric input of trace species to the world ocean, *Global Biogeochem. Cycles*, *5*, 193–259.

Dugdale, R. C., and F. P. Wilkerson (1998), Silicate regulation of new production in the equatorial Pacific upwelling, *Nature*, *391*, 270–273.

Ellwood, M. J. (2004), Zinc and cadmium speciation in subantarctic waters east of New Zealand, *Mar. Chem.*, *87*, 37–58.

Frew, R., A. Bowie, P. Croot, and S. Pickmere (2001), Nutrient and trace-metal geochemistry of an in situ iron-induced Southern Ocean bloom, *Deep Sea Res., Part II*, *48*, 2467–2481.

Frew, R. D., D. A. Hutchins, S. Nodder, S. Sanudo-Wilhelmy, A. Tovar-Sanchez, and P. W. Boyd (2005), Particulate iron dynamics during FeCycle in subantarctic waters southeast of New Zealand, *Global Biogeochem. Cycles*, doi:10.1029/2005GB002558, in press.

Fuhrman, J. A., R. W. Eppley, A. Hagstrom, and F. Azam (1985), Diel variation in bacterioplankton, phytoplankton, and related parameters in the S. Californian Bight, *Mar. Ecol. Prog. Ser.*, *27*, 9–20.

Fung, I. Y., S. K. Meyn, I. Tegen, S. C. Doney, J. John, and J. Bishop (2000), Iron supply and demand in the upper ocean, *Global Biogeochem. Cycles*, *14*, 281–296.

Hesse, P. P. (1994), The record of continental dust from Australia in Tasman Sea sediments, *Q. Sci. Rev.*, *13*, 257–272.

Hutchins, D. A., and K. W. Bruland (1994), Grazer-mediated regeneration and assimilation of Fe, Zn and Mn from planktonic prey, *Mar. Ecol. Prog. Ser.*, *110*, 259–269.

Hutchins, D. A., and K. W. Bruland (1998), Iron-limited diatom growth and Si:N uptake ratios in a coastal upwelling regime, *Nature*, *393*, 561–564.

Hutchins, D. A., G. R. DiTullio, and K. W. Bruland (1993), Iron and regenerated production: Evidence for biological iron recycling in two marine environments, *Limnol. Oceanogr.*, *38*, 1242–1255.

Hutchins, D. A., W.-X. Wang, and N. S. Fisher (1995), Copepod grazing and the biogeochemical fate of diatom iron, *Limnol. Oceanogr.*, *40*, 989–994.

Hutchins, D. A., G. R. DiTullio, Y. Zhang, and K. W. Bruland (1998), An iron limitation mosaic in the California upwelling regime, *Limnol. Oceanogr.*, *43*, 1037–1054.

Jickells, T. D. (1999), The inputs of dust derived elements to the Sargasso Sea: A synthesis, *Mar. Chem.*, *68*, 5–14.

Jickells, T. D., and L. J. Spokes (2001), Atmospheric iron inputs to the oceans, in *The Biogeochemistry of Iron in Seawater*, edited by D. Turner and K. A. Hunter, pp. 85–122, John Wiley, Hoboken, N. J.

Jickells, T. D., et al. (2005), Global iron connections between desert dust, ocean biogeochemistry and climate, *Science*, *308*, 67–71.

Johnson, K. S., R. M. Gordon, and K. H. Coale (1997), What controls dissolved iron concentrations in the world ocean?, *Mar. Chem.*, *57*, 37–161.

Karl, D. M., et al. (2003), Temporal studies of Biogeochemical processes determined from ocean time-series observations during the JGOFS era, in *Ocean Biogeochemistry: The Role of the Ocean Carbon Cycle in Global Change*, edited by M. J. R. Fasham, pp. 239–267, Springer, New York.

Kim, D.-O., K. Lee, S.-D. Choi, H.-S. Kang, J.-Z. Zhang, and Y.-S. Chang (2005), Determination of diapycnal diffusion rates in the upper thermocline in the North Atlantic Ocean using sulfur hexafluoride, *J. Geophys. Res.*, *110*, C10010, doi:10.1029/2004JC002835.

Kirchman, D. L. (1996), Microbial ferrous wheel, *Nature*, *383*, 303–304.
Law, C. S., A. J. Watson, M. I. Liddicoat, and T. Stanton (1998), Sulphur hexafluoride as a tracer of biogeochemical and physical processes in an open-ocean iron fertilisation experiment, *Deep Sea Res., Part II*, *45*, 977–994.
Law, C. S., A. P. Martin, M. I. Liddicoat, A. J. Watson, K. J. Richards, and E. M. S. Woodward (2001), A Lagrangian SF_6 tracer study of an anticyclonic eddy in the North Atlantic: Patch evolution, vertical mixing and nutrient supply to the mixed layer, *Deep Sea Res., Part II*, *48*, 705–724.
Law, C. S., E. R. Abraham, A. J. Watson, and M. I. Liddicoat (2003), Vertical eddy diffusion and nutrient supply to the surface mixed layer of the Antarctic Circumpolar Current, *J. Geophys. Res.*, *108*(C8), 3272, doi:10.1029/2002JC001604.
Levasseur, S., M. Frank, J. R. Hein, and A. N. Halliday (2004), The global variation in the iron isotope composition of marine hydrogenetic ferromanganese deposits: Implications for seawater chemistry?, *Earth Planet. Sci. Lett.*, *224*, 91–105.
MacIntyre, S. (1998), Turbulent mixing and resource supply to phytoplankton, in *Physical Processes in Lakes and Oceans*, *Coastal Estuarine Stud.*, vol. 54, edited by J. Imberger, pp. 539–567, AGU, Washington, D. C.
Maldonado, M. T., R. F. Strzepek, S. Sander, and P. W. Boyd (2005), Acquisition of iron bound to strong organic complexes, with different Fe binding groups and photochemical reactivities, by plankton communities in Fe-limited subantarctic waters, *Global Biogeochem. Cycles*, *19,* GB4S23, doi:10.1029/2005GB002481.
Martin, J. H., R. M. Gordon, S. Fitzwater, and W. W. Broenkow (1989), VERTEX: Phytoplankton/iron studies in the Gulf of Alaska, *Deep Sea Res.*, *36*, 649–680.
McKay, R. M. L., W. Wilhelm, J. Hall, D. A. Hutchins, M. M. D. Al-Rshaidat, C. E. Mioni, S. Pickmere, D. Porta, and P. W. Boyd (2005), Impact of phytoplankton on the biogeochemical cycling of iron in subantarctic waters southeast of New Zealand during FeCycle, *Global Biogeochem. Cycles*, *19,* GB4S24, doi:10.1029/2005GB002482.
McNeil, C. L., and D. M. Farmer (1995), Observations of the influence of diurnal convection on upper ocean dissolved-gas measurements, *J. Mar. Res.*, *53*, 151–169.
McTainsh, G. H. (1998), Dust storm index, in Sustainable agriculture: Assessing Australia's recent performance–A report of the National Collaborative Project on Indicators for Sustainable Agriculture, *SCARM Tech. Rep. 70*, pp. 65–72, Standing Comm. on Agric. and Resour. Manage., Victoria, Australia.
Middleton, N. J. (1984), Dust storms in Australia, frequency, distribution and seasonality, *Search*, *15*, 46–47.
Mioni, C. E., A. M. Howard, J. M. DeBruyn, N. G. Bright, M. R. Twiss, B. M. Applegate, and S. W. Wilhelm (2003), Characterization and field trials of a bioluminescent bacterial reporter of iron bioavailability, *Mar. Chem.*, *83*, 31–46.
Mioni, C. E., S. M. Handy, M. J. Ellwood, M. R. Twiss, R. M. L. McKay, P. W. Boyd, and S. W. Wilhelm (2005), Tracking changes in bioavailable Fe within SF_6 labeled HNLC waters: A first estimate using a heterotrophic bacterial bioreporter, *Global Biogeochem. Cycles, 19,* GB4S25, doi:10.1029/2005GB002476.
Morel, F. M. M., and N. M. Price (2003), The biogeochemical cycles of trace metals in the oceans, *Science*, *300*, 944–947.
Murray, J. W., J. N. Downs, S. Strom, C.-L. Wei, and H. W. Jannasch (1989), Nutrient assimilation, export production and 234 Thorium scavenging in the eastern equatorial Pacific, *Deep Sea Res.*, *36*, 1471–1489.
Nodder, S. D., and B. L. Alexander (1999), The effects of multiple trap spacing, baffles and brine volume on sediment trap collection efficiency, *J. Mar. Res.*, *57*, 1–23.
Nodder, S. D., P. W. Boyd, S. M. Chiswell, M. Pinkerton, and M. Greig (2005), Temporal coupling between surface and deep-ocean biogeochemical processes in two contrasting subtropical and subantarctic water masses, southwest Pacific Ocean, *J. Geophys. Res.*, *110,* C12017, doi:10.1029/2004JC002833.
Parekh, P., M. J. Follows, and E. Boyle (2004), Modeling the global iron cycle, *Global Biogeochem. Cycles*, *18*, GB1002, doi:10.1029/2003GB002061.
Price, N. M., and F. M. M. Morel (1998), Biological cycling of iron in the ocean, in *Metal Ions in Biological Systems*, vol. 35, *Iron Transport and Storage in Micro-organisms, Plants and Animals*, pp. 1–36, CRC Press, Boca Raton, Fla.
Richardson, K. M., M. H. Pinkerton, P. W. Boyd, M. P. Gall, J. Zeldis, M. D. Oliver, and R. J. Murphy (2004), Validation of SEAWIFS data from around New Zealand, *Adv. Space Res.*, *33*, 1160–1167.
Rue, E. L., and K. W. Bruland (1997), The role of organic complexation on ambient iron chemistry in the equatorial Pacific Ocean and the response of a mesoscale iron addition experiment, *Limnol. Oceanogr.*, *42*, 901–910.
Sedwick, P. N., P. R. Edwards, D. J. Mackey, F. B. Griffiths, and J. S. Parslow (1997), Iron and manganese in surface waters of the Australian subantarctic region, *Deep Sea Res., Part I*, *44*, 1239–1252.
Sherrell, R. M., and E. A. Boyle (1992), The trace metal composition of suspended particles in the oceanic water column near Bermuda, *Earth Planet. Sci. Lett.*, *111*, 155–174.
Sieburth, J. M., V. Smetacek, and J. Lenz (1978), Pelagic ecosystem structure: Heterotrophic compartments of plankton and their relationship to plankton size fraction, *Limnol. Oceanogr.*, *23*, 1256–1263.
Stegmann, P. M., and N. W. Tindale (1999), Global distributions of aerosols over the open ocean as derived from the coastal zone color scanner, *Global Biogeochem. Cycles*, *13*, 383–397.
Strom, S. L., C. B. Miller, and B. W. Frost (2000), What sets lower limits to phytoplankton stocks in high nitrate, low chlorophyll regions of the open ocean, *Mar. Ecol. Prog. Ser.*, *193*, 19–31.
Strzepek, R. F., M. T. Maldonado, J. Higgins, J. Hall, S. W. Wilhelm, K. Safi, and P. W. Boyd (2005), Spinning the "Ferrous Wheel": The importance of the microbial community in an iron budget during the FeCycle experiment, *Global Biogeochem. Cycles, 19,* GB4S26, doi:10.1029/2005GB002490.
Tortell, P. D., M. T. Maldonado, and N. M. Price (1996), The role of heterotrophic bacteria in iron-limited ocean ecosystems, *Nature*, *383*, 330–332.
Tortell, P. D., M. T. Maldonado, J. Granger, and N. M. Price (1999), Marine bacteria and biogeochemical cycling of iron in the oceans, *FEMS Microbiol. Ecol.*, *29*, 1–11.
Tovar-Sanchez, A., S. A. Sañudo-Wilhelmy, M. Garcia-Vargas, R. S. Weaver, L. C. Popels, and D. A. Hutchins (2003), A trace metal clean reagent to remove surface-bound iron from marine phytoplankton, *Mar. Chem.*, *82*, 91–99.
Turner, S. M., M. J. Harvey, C. S. Law, P. D. Nightingale, and P. S. Liss (2004), Iron-induced changes in oceanic sulfur biogeochemistry, *Geophys. Res. Lett.*, *31*, L14307, doi:10.1029/2004GL020296.
Twining, B. S., S. B. Baines, and N. S. Fisher (2004a), Element stoichiometries of individual plankton cells collected during the Southern Ocean Iron Experiment (SOFeX), *Limnol. Oceanogr.*, *49*, 2115–2128.
Twining, B. S., S. B. Baines, N. S. Fisher, and M. R. Landry (2004b), Cellular iron contents of plankton during the Southern Ocean Iron Experiment (SOFeX), *Deep Sea Res., Part I*, *51*, 1827–1850.
Varela, D. E., and P. J. Harrison (1999), Seasonal variability in nitrogenous nutrition of phytoplankton assemblages in the northeastern subarctic Pacific Ocean, *Deep Sea Res., Part II*, *46*, 2505–2538.
Wilhelm, S. W., M. G. Weinbauer, C. A. Suttle, and W. H. Jeffrey (1998), The role of sunlight in the removal and repair of viruses in the sea, *Limnol. Oceanogr.*, *43*, 586–592.
Wu, J., and E. Boyle (2002), Iron in the Sargasso Sea: Implications for the processes controlling dissolved Fe distribution in the ocean, *Global Biogeochem. Cycles*, *16*(4), 1086, doi:10.1029/2001GB001453.
Yoshida, T., K. Hayashi, and H. Ohmoto (2002), Dissolution of iron hydroxides by marine bacterial siderophore, *Chem. Geol.*, *184*, 1–9.

E. R. Abraham, M. Hadfield, P. Hill, C. S. Law, M. Oliver, M. Pinkerton, and M. Smith, National Institute of Water and Atmosphere, Greta Point, Wellington, New Zealand.

P. W. Boyd, National Institute of Water and Atmosphere Centre for Chemical and Physical Oceanography, Department of Chemistry, University of Otago, Dunedin, New Zealand. (p.boyd@niwa.co.nz)

P. L. Croot, Leibniz-Institut für Meereswissenschaften (IFM-GEOMAR), Düsternbrooker Weg 20, D-24105, Kiel, Germany.

M. Ellwood, J. Hall, S. Pickmere, and K. Safi, National Institute of Water and Atmosphere, Hillcrest, Hamilton, New Zealand.

R. D. Frew, K. A. Hunter, S. Sander, and R. Strzepek, Department of Chemistry, University of Otago, Dunedin, New Zealand.

S. Handy, C. Hare, D. A. Hutchins, and K. LeBlanc, College of Marine Studies, University of Delaware, Lewes, DE 19958, USA.

J. Higgins, C. Mioni, and S. W. Wilhelm, Department of Microbiology, University of Tennessee, Knoxville, TN 37996-0845, USA.

M. T. Maldonado, Department of Earth and Ocean Sciences, University of British Columbia, Vancouver V6T 1Z4, BC, Canada.

R. M. McKay, Department of Biological Sciences, Bowling Green State University, Bowling Green, OH 43403, USA.

S. A. Sanudo-Wilhelmy, Marine Sciences Research Center, Stony Brook University, Stony Brook, NY 11794-5000, USA.

A. Tovar-Sanchez, Instituto Mediterraneo de Estudios Avanzados (IMEDEA), Esporles E-07170, Mallorca, Spain.